



Generative Design Method of Building Group Based on AIP (Aging in Place) Assessment: The Case of Dense Urban Renewal Districts in Hong Kong

35

Youlong Gu, Yecheng Zhang,
and Wei Xuan

Abstract

High-density urban development is often accompanied by the phenomenon of aging, and AIP (aging in place) is considered as one of the main approaches to cope with aging in high-density urban environments in the future. In this paper, we explore the possibility of building group generation at the scale of high-density urban blocks and the future guidance of urban design based on the AIP assessment system and a generative design method under multi-objective optimization. To achieve this goal, we take Sham Shui Po and its surrounding areas in Hong Kong as the study area, and then score the indicators at both the block and grid levels through the assessment system in the AIP context, and then obtain objective weights through the CRITIC method to obtain a comprehensive score. We further delineate the renewal area by the clustering algorithm, filter the generation range, and then use the indicators filtered based on the weights as the optimization direction to design a set of building generation patterns according to the local planning requirements and then carry out

multi-objective optimization generation design. The original gene data is extracted and analyzed after the results are verified to obtain a better range of indicators for the urban design. The evaluation results of the generated building groups show that the built environment of the block is more suitable for aging-friendly living and can guide future high-density urban design under this AIP assessment system according to the better gene range in the system.

Keywords

Aging in place • Urban renewal • Assessment system • Generative design method • CRITIC method • Multi-objective optimization • Hong Kong

35.1 Introduction

35.1.1 Background

Currently, the pace of population aging is much faster than in the past. WHO states that between 2015 and 2050, the proportion of the world's population over 60 years will nearly double from 12 to 22% (World Health Organization 2022). Thus, aging will be a national health and social system challenge for all countries and regions in the future.

In recent years, AIP (aging in place) has been recognized as a good old-age care approach that

Y. Gu · Y. Zhang · W. Xuan (✉)
Hefei University of Technology, Hefei, China
e-mail: xuanwei417@163.com

Y. Gu
e-mail: gylreuben@gmail.com

enables older people to maintain independence and have access to social support. There is a growing emphasis on the role of the local environment in facilitating AIP, which is reflected in debates around lifetime neighborhoods, livable communities, and age-friendly cities (Buffel et al. 2018; Scharlach and Lehning 2013). At the same time, some research adds to our understanding of how to create communities that support the needs of people as they age, including adapting to the physical environment (e.g., infrastructure, transportation, and housing) as well as social dimensions (e.g., social and civic engagement, community care, and neighborhood support) (Buffel et al. 2019; Gardner 2011).

In terms of conceptual discovery and spatial identification related to the aging place, Lewis and Buffel (2020) also compared in detail the conceptual differences between aging in place and the places of aging through case studies, and explore the process of change over time. Dawidowicz et al. (2020) used contemporary trends in the field, state and local policy, as well as on survey data from the target population and on information provided by experts to identify active aging places based on the QGIS platform.

In the context of research on aging in place, some studies have assessed and scored the living space of older adults through an evaluation system designed based on AIP. For example, Mercader-Moyano et al. (2020) (Mercader-Moyano et al. 2020) proposed a Multidimensional Assessment System of the Built Environment (MASBE) to test the built environment, which emphasizes the acceptance and perceived suitability of housing and neighborhood size for older adults. By designing and quantifying 35 multidisciplinary variables related to the needs of the elderly through seven categories of dimensions, a new evaluation model is provided for decision makers to help adjust future urban policies. Fan Zhang et al. (2021) (Zhang et al. 2021) propose a multi-scale spatial framework for housing that uses BIM information to support multi-level spatial evaluation to assist the government in assigning suitable public housing to elderly applicants, and to provide property

developers and local governments with additional guidelines for housing design and urban redevelopment.

35.1.2 Our Study

Most AIP-based quantitative assessment systems involve multiple levels of complex data, and the lack of actual BIM information for buildings in some areas due to their early age, or the difficulty of obtaining information related to the building interior environment due to personal privacy and the actual living environment, makes it difficult to implement the entire assessment system completely and quickly. At the same time, the resulting score results are not translated into spatial terms, which is difficult for developers or governments to understand.

Therefore, in order to reduce the difficulty of spatial information acquisition, this paper designs a set of AIP assessment systems based on multiple sources of big data from meso perspectives combined with literature review, and generates multi-objective optimization of building groups based on the assessment results, and translates the results into spatial terms to better help architects, urban planners and policy makers to understand and formulate urban renewal plans.

Like other developed countries and regions, Hong Kong is facing a serious population aging challenge. As the area with the highest population density in Hong Kong, Sham Shui Po and its surrounding areas will achieve rapid growth of more than 10% in the official population forecast for the next 10 years (Planning Department 2021). This presents a challenge to further improve the living environment while addressing the persistent issue of aging. Jayantha et al. (2018) also pointed out that the structural design and configuration of facilities in rental housing in Sham Shui Po are not reasonable and the government needs to redesign the physical environment space. Therefore, we choose the dense urban renewal districts of Sham Shui Po as the case study.

This paper is organized as follows: Sect. 35.2 describes the complete workflow of the study,

including the AIP assessment system, data acquisition, weight acquisition, region delineation, and strategy of the evolutionary algorithm; Sect. 35.3 describes the generated results, visualizes the outstanding individuals, and validates the results on this basis, and extracts the raw genetic data as a spatial terminology guide; finally, Sect. 35.4 summarizes the main conclusions of this paper.

35.2 Material and Methods

In terms of site selection, the physical space of Sham Shui Po and the surrounding area in Hong Kong which is a representative of high-density cities, and where there is a serious aging problem, is chosen as the site for the research. Sham Shui Po (longitude: 114.167210, latitude: 22.328171) is located in the north-western part of the Kowloon Peninsula, covering an area of about 1047 hectares, with a population of about 353,000, divided into 21 constituencies. As early as 2000 onward, the government attempted to incorporate some specific elements of facility and housing design consistent with the aging in place concept into its public housing rebuilding program to meet the needs of older adults.

We designed a generative method-focused research workflow for the generation and optimization of the overall environment for the area's physical space based on AIP shown in Fig. 35.1.

35.2.1 AIP Assessment Process

In terms of indicator construction, this research aims to analyze the information evaluation of community public facilities and transportation facilities for older people based on the meso-scale. Therefore, by researching the interaction between the physical family environment and old age through three indicators of safety, accessibility and mobility, and comfort, and stress the importance of time-series changes in the environment and place to the healthy aging through wind and heat environmental simulation data, and then judge the importance of multi-dimensional indicators by an objective weighting method, and constructs a scoring matrix to compare the weights of each indicator during the comprehensive multi-instrument evaluation.

35.2.1.1 AIP Assessment Process

The literature review was used for the assessment system establishment as well as preliminary screening work. The literature research data in this paper was obtained from 2015–2022 sciencedirect, springer, wiley and other databases, and keywords such as *aging in place*, *AIP*, and *place aging* were selected for the search, and more than 10 pieces of literature related to quantitative assessment and index construction were retrieved. Based on the multi-source big data acquisition method and feasibility analysis under the mesoscopic scale of this paper, the final

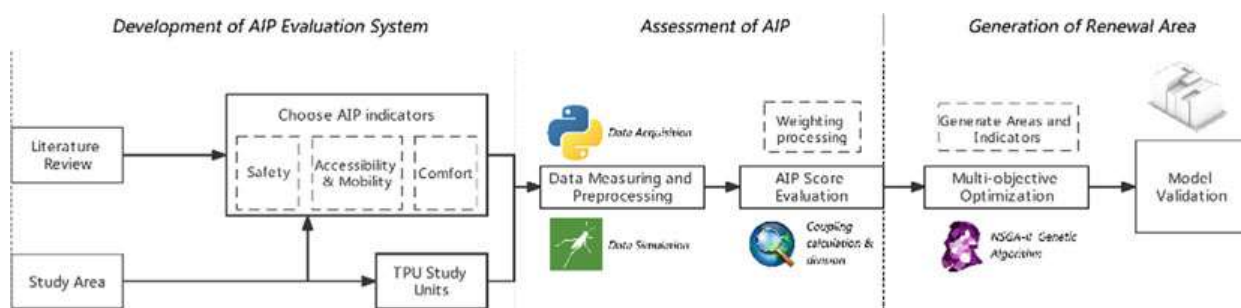


Fig. 35.1 Research workflow

Table 35.1 AIP indicator assessment system

Level	Indicators	Description	Source
Safety	Traffic flow	The suitability of traffic flow	(Jelokhani-Niaraki et al. 2019)
	Lighting at night	Street brightness rating at night	(Jelokhani-Niaraki et al. 2019)
	Security and police service	Number of emergency phone booths, police patrols, policy stations and other policy services within walking distance (500 m)	(Jelokhani-Niaraki et al. 2019)
Accessibility & Mobility	Entertainment facility	Number of parks, Greenery, sports facilities, community centers, and other recreational and sports facilities within a walking distance (500 m)	(Jelokhani-Niaraki et al. 2019); (Kano et al. 2018); (Luciano et al. 2020)
	Shopping facility	Number of grocery stores, markets, shopping centers, and other shopping facilities within walking distance (500 m)	(Kihl et al. 2005; Luciano et al. 2020)
	Medical facility	Number of pharmacies, pharmacies, community clinics, hospital clinics and other medical facilities within walking distance (500 m)	(Kihl et al., 2005; Luciano et al. 2020)
	Transportation facility	Number of bus stops, subway stations and other transportation facilities within walking distance (500 m)	(Jelokhani-Niaraki et al. 2019; Kano et al. 2018; Kihl et al., 2005; Luciano et al. 2020)
	General facility	Number of banks, laundries, bookstores, libraries and other transportation facilities within walking distance (500 m)	(Luciano et al. 2020)
Comfort	Solar radiation (winter)	Community-wide solar radiation in winter	(Giridharan et al. 2007); (Peng and Maing 2021)
	UTCI comfort	UTCI comfort outdoor environment	(Giridharan et al. 2007; Sining Peng et al. 2021)
	Pedestrian level wind	1.5 m mean wind speed numerical simulation	(Giridharan et al. 2007; Sining Peng et al. 2021)
	Integrated environment	Coupled humidity, wind speed and other integrated wind-thermal environment	(Giridharan et al. 2007; Sining Peng et al. 2021)

selection of 12 indicators for three levels of Safety, Accessibility & Mobility, and Comfort is shown in Table 35.1.

Considering the system accuracy requirements, this study uses the design of 10 M*10 M fishnet as the basic analysis unit in ArcGIS 10.8, and conducts sub-indicator evaluations based on the AIP evaluation framework. Among them, house price data and traffic flow intensity data are collected through Python 3.8, and security and police services, the accessibility & mobility of recreational facilities, shopping facilities, medical facilities, transportation facilities and general

facilities, are POI (point of interest), sourced from Hong Kong Geodata Store (<https://geodata.gov.hk/gs/>), and then accessibility analysis is performed by the radiation range through the proximity tool in ArcGIS 10.8. Average radiation in winter, thermal comfort, wind speed at pedestrian height and integrated wind-heat environment data are distributed for calculation and coupled by the free Grasshopper 3D Ladybug Tools.

The block-level division in this study is based on the grid-level basic score and the Hong Kong Small Tertiary Planning Unit Group. For the

purpose of urban planning, the entire territory of Hong Kong is divided into 291 Tertiary Planning Units (TPUs) by the Planning Department of the Government of the Hong Kong Special Administrative Region. The planning system incorporating the TPUs thus allows for a more localized and accurate assessment system and scope of generation, after the total grid score is obtained, the net is segmented based on the block area and the grid arithmetic mean within the area is calculated. AIP evaluation score of block level can be seen in Fig. 35.2.

35.2.1.2 Weight Acquisition

This study determines the weight contribution of each indicator mainly based on the information

entropy of the data set. The traditional entropy method can only calculate the entropy according to the variability of indicators but ignores the correlation between data. So, the CRITIC method is applied to make corrections, which comprehensively measures the objective weight of an indicator based on the comparative strength of the evaluation indicators and the conflict between indicators. By this method, the variability of the indicators is shown by a standard deviation of S_j (indicating the fluctuation of the differences in the values taken within each indicator). The larger standard deviation indicates that the greater the difference in the values of the indicator, the more the information will be screened, and the evaluation intensity of the

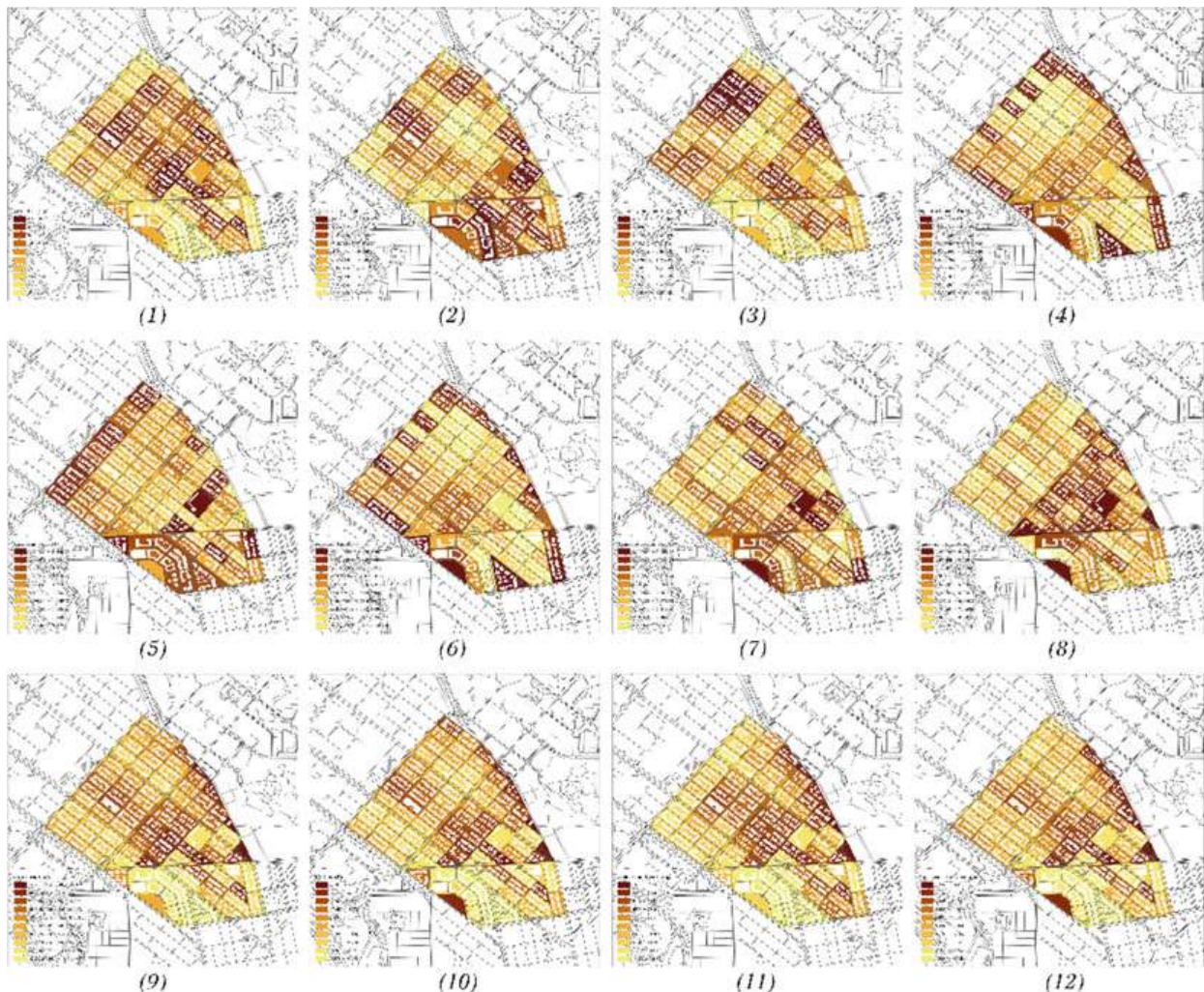


Fig. 35.2 AIP evaluation score of block level. (1) traffic flow (2) lighting at night (3) security and police service (4) entertainment facility (5) shopping facility (6) medical

facility (7) transportation facility (8) general facility (9) solar radiation (10) UTCI comfort (11) pedestrian level wind (12) integrated environment

indicator itself will be stronger, and more weight should be assigned to the indicator) and the conflicting of indicators is shown by a correlation coefficient (indicating the correlation between the indicators. If the correlation with other indicators is stronger, the conflict between the indicator and other indicators will be less, the more the same information will be screened, the more repetitive evaluation content can be reflected, weakening the evaluation intensity of the indicator to a certain extent, and less weight should be assigned to the indicator) (Table 35.2).

$$\left\{ \begin{array}{l} x = \frac{1}{n} \sum_{i=1}^n X_{ij} \\ S_j = \sqrt{\frac{\sum_{i=1}^n (X_{ij} - x)^2}{n-1}}; R_j = \sum_{i=1}^p (1 - r_{ij}) \end{array} \right.$$

35.2.1.3 Total Score Assessment and Zoning

After obtaining the weights, the scores of each index of the grid are weighted and calculated, and combined weighting and TPU planning range to obtain grid level and block level total scores as shown in Fig. 35.3.

Spatial clustering of scores by Anselin Local Moran's I is conducted to update generation

ranges (Zhang et al. 2019). The algorithm results in high-high clusters (HH), low-low clusters (LL), high-low outliers (HL) and low-high outliers (LH) at the 95% confidence level of statistical significance. The clustering at the block level and the grid level based on INVERSE_DISTANCE, corresponding to the low-low clustering areas from the significance test on the assessment system, and the comparative analysis excludes the indicator interference of house prices and general facilities. The final total scores of flow-low clustering areas are shown in the figure. After overlaying the TPU planning range, regional zoning is conducted by the evolutionary algorithm, and after removing the heterogeneous commercial plots, a total of 13 TPU composite commercial and residential plots are selected for the generating design level based on INVERSE_DISTANCE, corresponding to the low-low clustering areas from the significance test on the assessment system, and the comparative analysis excludes the indicator interference of house prices and general facilities. The final total scores of flow-low clustering areas are shown in the figure. After overlaying the TPU planning range, regional zoning is conducted by the evolutionary algorithm, and after removing

Table 35.2 Analysis results of the CRITIC method

Indicator	Variability of indicators	Conflict of indicators	Volume of information	Weight (%)
NMMS_traffic flow	0.157	11.449	1.799	7.032
NMMS_lighting	0.124	10.696	1.327	5.189
NMMS_security	0.204	11.823	2.406	9.405
NMMS_entertainment	0.199	11.987	2.386	9.327
NMMS_shopping	0.185	10.753	1.985	7.757
NMMS_medical	0.221	10.996	2.428	9.490
NMMS_transportation	0.167	10.846	1.816	7.097
NMMS_general	0.166	10.639	1.770	6.918
MMS_solar	0.254	12.012	3.049	11.920
MMS_utci comfort	0.255	12.059	3.077	12.028
MMS_wind	0.125	10.965	1.368	5.347
MMS_environment	0.203	10.688	2.172	8.490

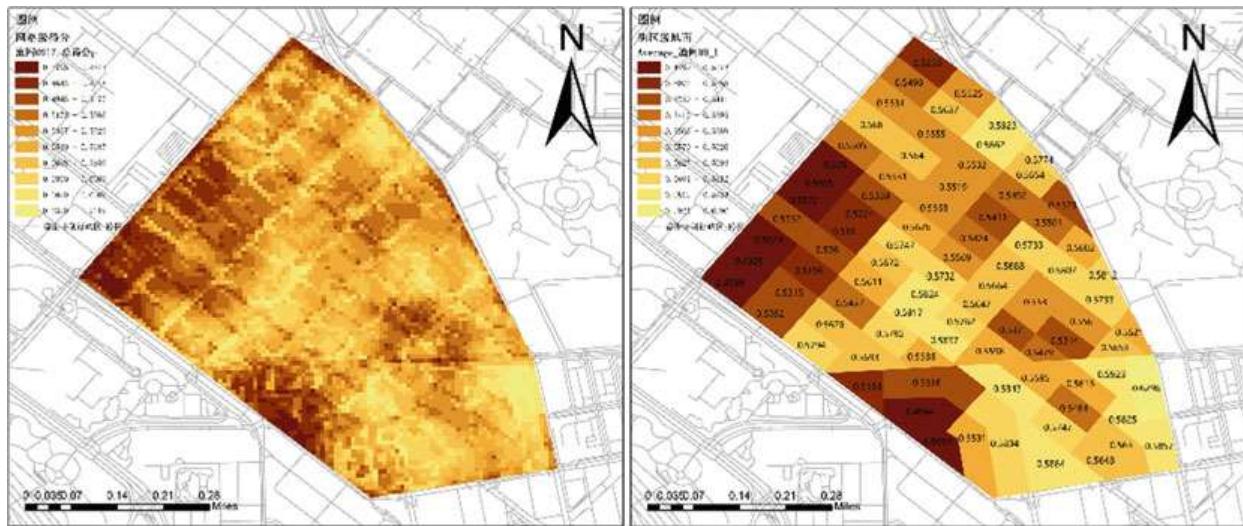


Fig. 35.3 Total score at the grid level (Left) and total score at the TPU block level (Right)

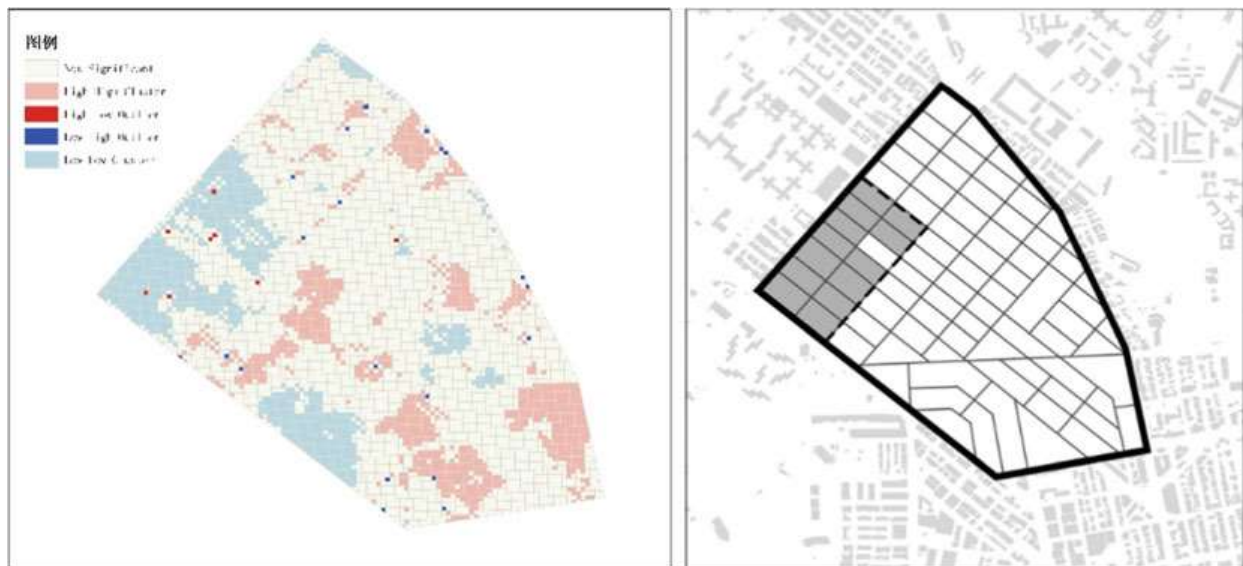


Fig. 35.4 Anselin Local Moran's: Distribution of clustering results (Left) and zoning of generation regions (Right)

the heterogeneous commercial plots, a total of 13 TPU composite commercial and residential plots are selected for the generating design (Fig. 35.4).

35.2.2 Generative Design Method

35.2.2.1 Building Generation Settings

In this study, we hope to be able to control simple geometric parameters to simulate the complex changes of Hong Kong's urban blocks, and to achieve basic parameter adjustment through the plug-in Grasshopper in the 3D-

NURBS modeling software Rhinoceros 3D. According to the survey of the study area, we divide the base grid by the random rectangular tiling method, take the building footprint of the original plot as a guiding parameter to control the rectangular tiling subdivisions, and conduct random subdivision by Jared Tarbell textures under the subdivision conditions, and then obtain the building base grid through random distance setbacks. According to the current situation of the study area, grids are deleted with the two values of $10m^2$ and $1000m^2$ as filtering conditions, to remove the building substrate with scale



Fig. 35.5 Diagram of plot generation (1) Zoning based on original substrate (2) Zoning (3) Texture subdivision (4) Plot setback (5) Plot screening

distortion and simulate the small spaces in the local block. After obtaining the final substrate, building density control is carried out according to the Hong Kong Planning Standards and Guidelines (Planning Department 2021). According to the Planning Department's classification conditions, the planning area falls into Residential Development Density Zone 1, with a maximum residential plot ratio of 8.00, and the building height is controlled to 40-60 m through spatial calculations and development planning, and the final building form will be randomly extruded within the range of the final substrate (Fig. 35.5).

For this generation process, there are following variables as genes:

- Plot horizontal partitioning in the long side direction (Hereinafter referred to as x division, range 2–4)
- Plot horizontal partitioning in the short side direction (Hereinafter referred to as y division, range 1–3)
- Plot random subdivision level (Hereinafter referred to as subdivide, range 1–3)
- Setback distance of plot substrate (Hereinafter referred to as concession, range 5–10%)
- Plot building height (Hereinafter referred to as height, range 40–60 m)

35.2.2.2 Evolutionary Strategy

Multi-objective optimization based on the evolutionary algorithm applied in this study is NSGA-2 developed by (Deb et al. 2000) as a driver algorithm of the free Grasshopper 3D Wallacei plugin developed by Mohammed Makki, (Makki et al. 2018).

The CRITIC method ranks the contribution of the constructed AIP indicators, ensuring the accuracy and efficiency of the algorithm at the same time. In this study, the top five indicators ranked by the CRITIC method are selected for the generation setting, namely thermal comfort, average radiation in winter, security and police services, accessibility and mobility of medical facilities and accessibility and mobility of recreational facilities, covering 53% of the interpretation weight and meeting the system assessment requirements, according to which the constraints and objectives are set in Grasshopper 3D.

Hong Kong has a subtropical monsoon climate. In addition, the deep valley-like environment caused by the small building space in the study area leads to poor ventilation, and thus

thermal comfort becomes an important indicator of assessing the outdoor thermal environment. Therefore, the maximum thermal comfort (UTCI) is selected as the suitability criterion by numerical analysis with the Grasshopper 3D Ladybug Tools.

The dense and homogeneous building layout of the study area is prone to produce building shadows and radiation shading in winter, which is not conducive to the daily outdoor activities of older people. As a result, the period from the autumn equinox (9.23) to the spring equinox (3.23) is selected for the analysis of solar radiation with the Grasshopper 3D Ladybug Tools, to select the maximum average radiation in winter as the suitability criterion.

Security and police services mainly cover the number of emergency phone booths, patrol police, policy stations and other policy services within a 500 m walking distance. The analysis model replaces accessibility and mobility equivalents by the maximum building area within a 500 m walking distance and the maximum accessibility and mobility is selected as the suitability criterion.

The accessibility and mobility of medical facilities mainly covers the number of medical facilities including pharmacies, drugstores, community clinics and hospital outpatient clinics within a 500 m walking distance. The analysis model replaces accessibility and mobility equivalents by the maximum building area within a 500 m walking distance and the maximum accessibility and mobility is selected as the suitability criterion.

The accessibility and mobility of entertainment facilities mainly covers the number of parks, green spaces, sports facilities, community centers and other recreational and sports facilities within a 500 m walking distance. The analysis model replaces accessibility and mobility equivalents by the maximum building area within a 500 m walking distance and the maximum accessibility and mobility is selected as the suitability criterion.

Points related to medical facilities and recreational facilities are derived from building data, and the spatial location of such points is

unchanged by default in the generated analysis, i.e., the spatial location is ensured to be physically covered in the generation of the building substrate.

The NSGA-2 parameters in this study are set to a generation size of 50, a generation count of 100, a total population size of 5000, a crossover probability of 0.9 and a mutation probability of 1/n.

35.3 Results

35.3.1 Simulation Results

Four basic types of diagrams of Wallacei reflect the strengths and weaknesses of the global analysis results (Fig. 35.6). Coupling analysis is conducted between the Standard Deviation (SD) Diagram with the Standard Deviation Trendline (SDT), with red lines standing for the first generation and blue lines for the last generation. The center line of each SD curve indicates the average fitness value for a generation. Throughout most of the simulation run, the five indicators under the optimization change in a clear and consistent trend. The center line moving towards the optimal direction from the first to the last generation, with the objectives basically in a stable or increasing state, and the convergence between the optimization objectives observed in the final generations indicates that the algorithm converges to optimality at the end of the simulation.

The Fitness Value Diagram (FV) and Mean Value Trendline Diagram (MVT) can be used to examine the fitness of individuals in parallel (2018) (Navarro-Mateu et al. 2018), with red lines standing for the first generation and blue lines for the last generation. It can be observed that in the Fitness Value Diagram, individuals present gradual convergence and an increase in scores, indicating that more fit individuals are generated during the simulation process. For the indicators of maximum medical and maximum police in the Mean Value Trendline Diagram, the average score shows a partial decrease during the convergence, inconsistent with the other

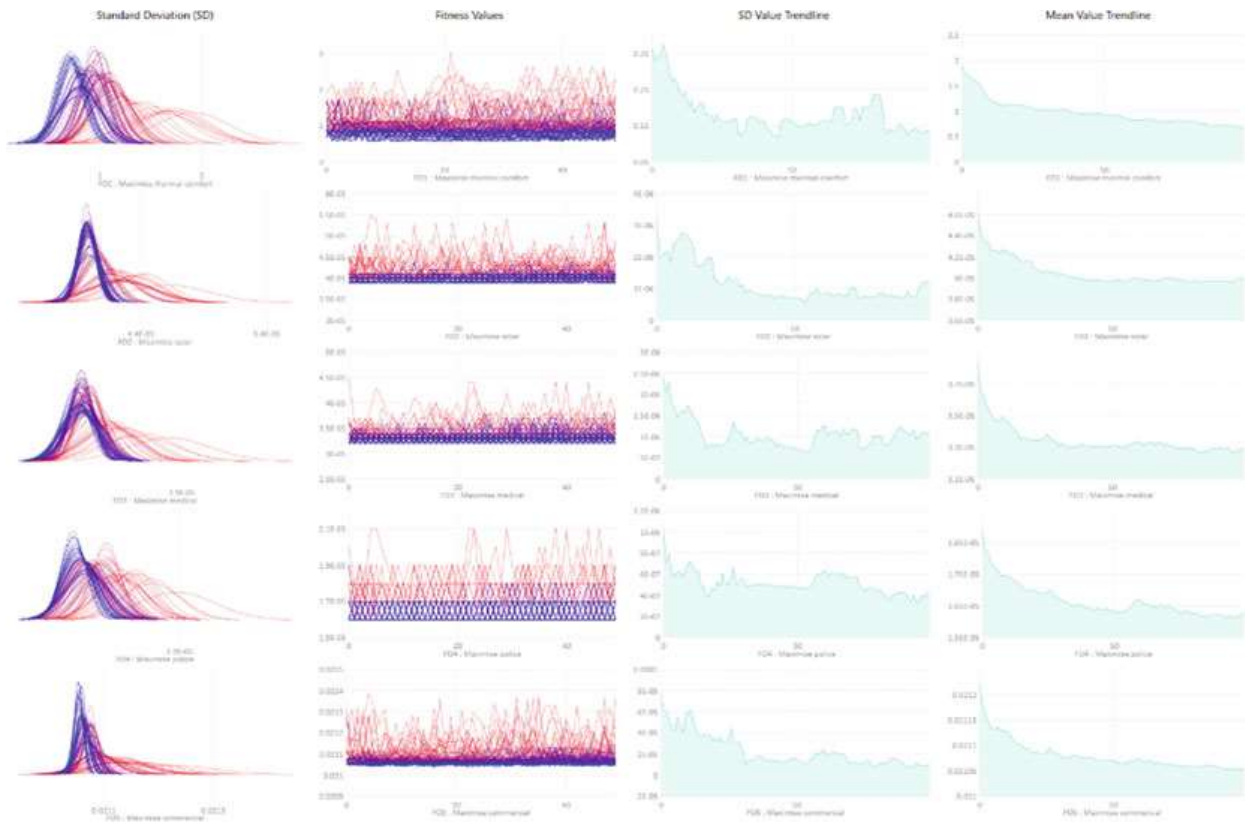


Fig. 35.6 Simulation results (From left to right, SD, FV, SDT, MVT)

indicators and demonstrates the need for the analysis of the global 5000 individuals, with 5000 iterations of the design problem showing an uneven pattern across the simulation and helping to find the better solution.

- (1) Fitness Average: (x_n means the ranking of solution values according to a specific fitness criterion).

$$FA = \frac{x_1 + x_2 + x_3 + x_4 + \dots + x_n}{n}$$

- (2) Pareto Front: selected by the K-means clustering algorithm in the last generation (99th generation) according to the clustering center solution.

The selection of the fitness average reflects the phenotype of the highest average score for all indicators, but may introduce extreme individuals specific to the indicator, allowing individuals to achieve a higher average ranking by weakening other indicator scores, while the Pareto representative solution allows the selection of the best phenotype for the relative relationship of a single indicator. For the former, the Parallel

35.3.2 Excellent Individuals Selection

Due to the strategic nature of the high-density solution scheme in the evolutionary algorithm, a large number of solutions are output as the final result during each iteration, thus it is especially critical to conduct the final individual selection and the statistical analysis of the global solution data. In phenotype selection, careful consideration needs to be made on the way genes are remapped, to make the final solution close to the significant correlation.

On this basis, two types of selection models are used for phenotype selection in this study:

Coordinate Plot is used to filter the top three individuals of 99–19, 92–24 and 98–23. For the latter, the unsupervised machine learning algorithm K-means is used for clustering analysis, with three clusters, in which the central cluster is selected as the representative solution, and the three individuals are 99–0, 99–8 and 99–16. The original genes are obtained on the basis of representational extraction, and since the number of buildings generated in a single block at a time is random, the original genes of the individual in a single block and full blocks are reflected by the calculated arithmetic mean (Fig. 35.7, Table 35.3).

$$X_G = \frac{x_1 + x_2 + x_3 + x_4 + \dots + x_{13}}{13}$$

(x_n means the arithmetic mean value of a particular type of gene in a single block)

In this simulation, the top three individual results selected based on the fitness average cover the higher scoring results for each indicator score, basically achieving the optimal combined average while satisfying the high value of each indicator. The three individuals selected from each gene series reflect high consistency in terms of random subdivision level, substrate setback

distance and building height, and therefore one of the optimal solutions for each gene series can be obtained (Fig. 35.8, Table 35.4).

The three types of Pareto front solutions filtered by K-means represent the three types of generative results in the last generation with certain variability, provided that the Pareto front is achieved, generating greater variability in genes as well as in phenotypes when being compared with fitness averages, and the generative models provide a visual representation comparison of model generation results in the 99th generation.

35.3.3 Results Verification

The six types of results based on the fitness average and the Pareto front are validated in the model, and the coupled calculation of regenerated block scores is conducted in ArcGIS 10.8 by physical engine simulation and data collection, to maintain the weight contribution of each indicator constant and summarize the total and arithmetic mean scores of the 13 blocks in the renewal area for comparison with the original scores (Figs. 35.9, 35.10).

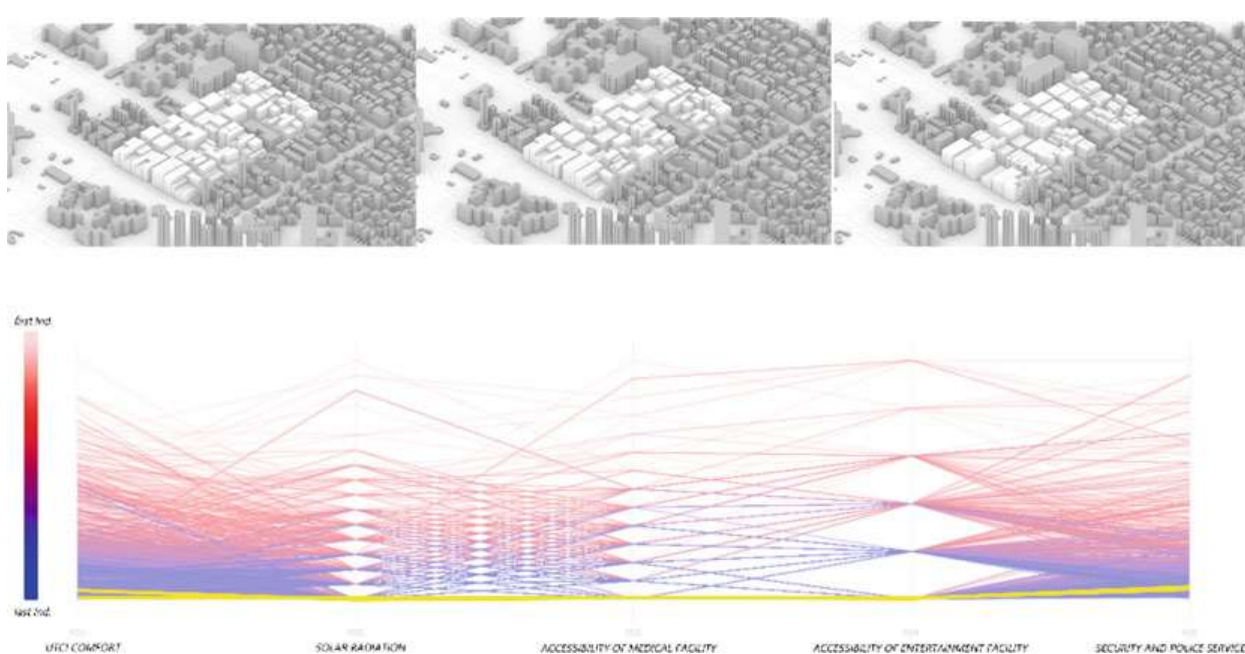
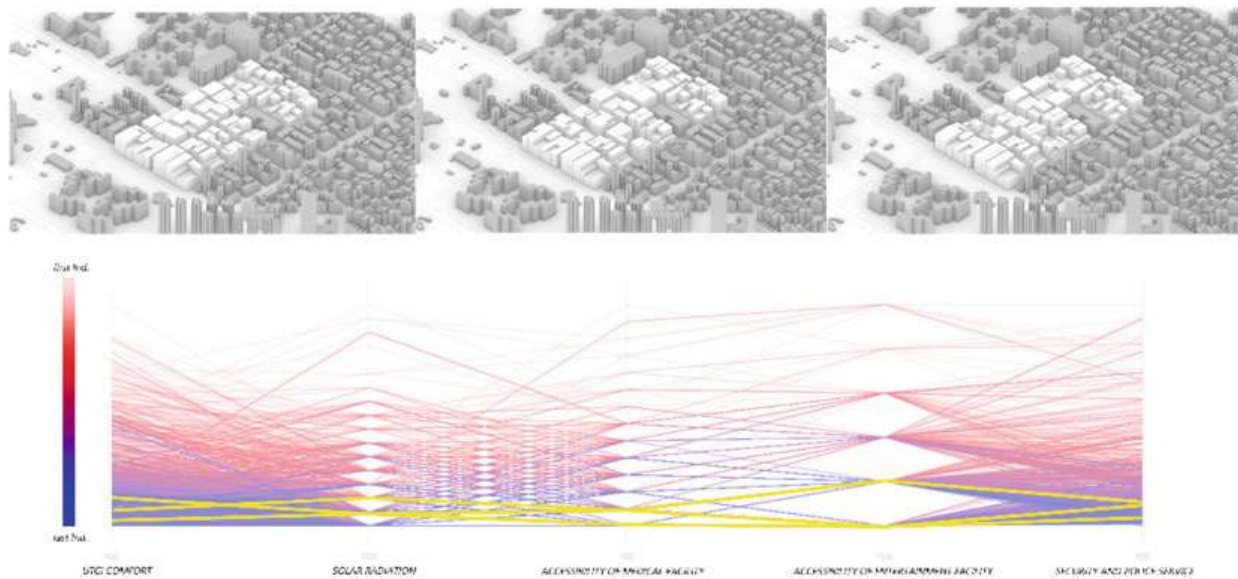


Fig. 35.7 Corresponding generation results (Left, middle, right) and PCP Lines for the three individuals of 99–19, 92–24 and 98–23

Table 35.3 Corresponding initial genes for the three individuals of 99–19, 92–24 and 98–23

	Gen.99 Ind.19	Gen.92 Ind.24	Gen.98 Ind.23
X division	3.08	3.00	3.15
Y division	2.23	2.15	1.85
Subdivide	2.13	2.08	2.13
Concession	0.93	0.93	0.93
Height	56.62	58.00	56.37

**Fig. 35.8** Corresponding generation results (Left, middle, right) and PCP Lines for the three individuals of 99–0, 99–8 and 99–16**Table 35.4** Corresponding initial genes for the three individuals of 99–0, 99–8 and 99–16

	Gen.99 Ind.0	Gen.99 Ind.8	Gen.99 Ind.16
X division	2.92	3.00	3.23
Y division	2.00	2.15	1.92
Subdivide	1.99	2.13	1.95
Concession	0.93	0.93	0.93
Height	56.68	57.52	56.83

Similar to the Parallel Coordinate Plot results, the three individuals selected based on the fitness average show better results in terms of mean total scores, with less variation in mean scores. Each block follows essentially the same trend, with the highest increase in total score of 0.0381 and the lowest increase of 0.0361, an average increase of

about 0.0373 and significant increases in blocks 1, 3, 10 and 13. The three individuals selected on the basis of Pareto front improve their total score by a maximum of 0.0322, a minimum of 0.0257 and an average of about 0.0290, while having certain variations in the trend of score improvement (Tables 35.5, 35.6).

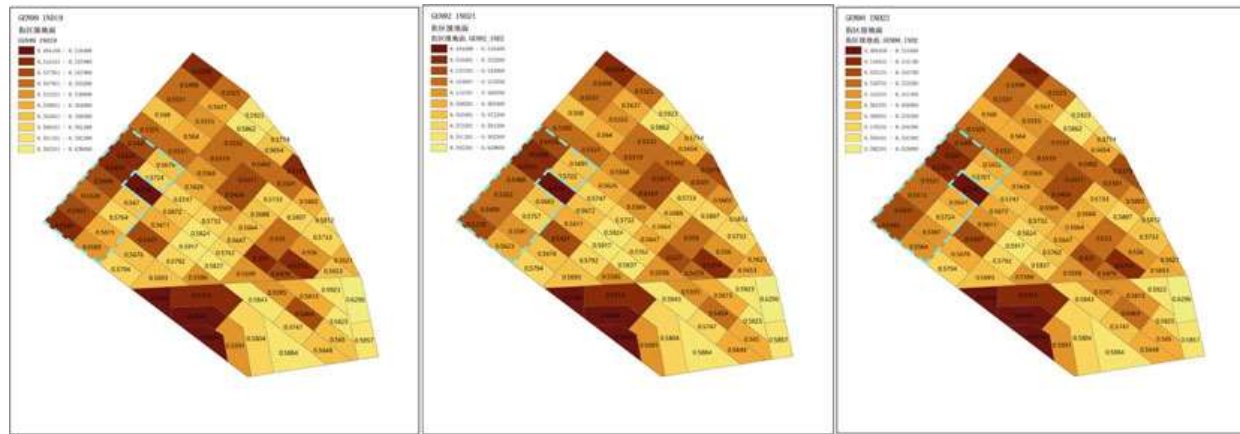


Fig. 35.9 Corresponding AIP assessment results of the three excellent individuals of 99–19, 92–24 and 98–23

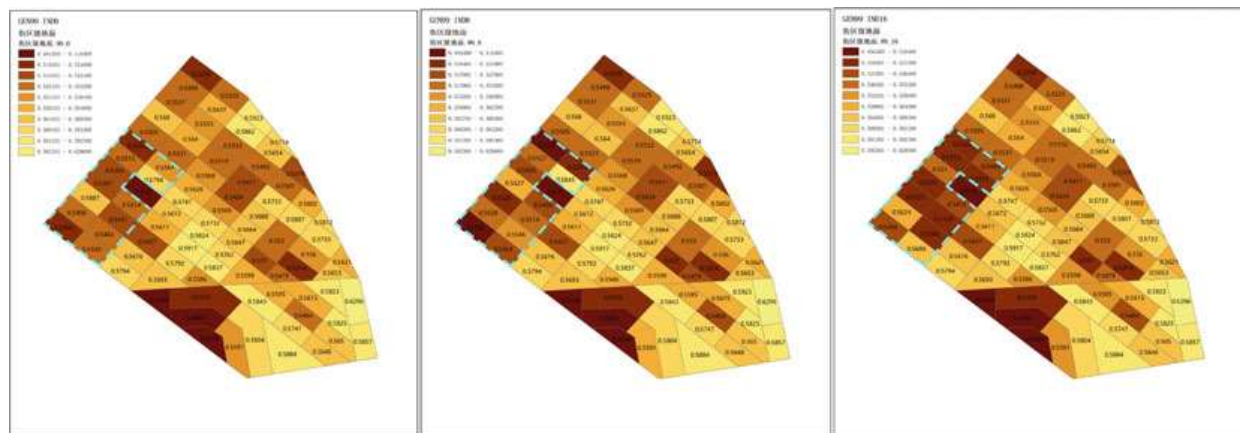


Fig. 35.10 Corresponding AIP assessment results of the three excellent individuals of 99–0, 99–8 and 99–16

Table 35.5 Corresponding AIP scores of the renewal plots for the three excellent individuals of 99–19, 92–24 and 98–23

PLOT	ORIGIN	GEN99_IND19	GEN92_IND24	GEN98_IND23
1	0.4799	0.5346	0.5378	0.5392
2	0.4929	0.5451	0.5499	0.5431
3	0.5024	0.5528	0.5502	0.5515
4	0.5332	0.5468	0.5488	0.5521
5	0.5072	0.5372	0.5322	0.5331
6	0.5050	0.5431	0.5440	0.5405
7	0.5005	0.5325	0.5298	0.5320
8	0.5392	0.5589	0.5623	0.5564
9	0.5315	0.5615	0.5591	0.5587
10	0.5196	0.5764	0.5757	0.5724
11	0.5360	0.5670	0.5685	0.5647
12	0.5389	0.5679	0.5697	0.5652
13	0.5224	0.5724	0.5722	0.5701
Average	0.5161	0.5536	0.5539	0.5522

Table 35.6 Corresponding AIP scores of the renewal plots for the three excellent individuals of 99–0, 99–8 and 99–16

PLOT	ORIGIN	GEN99_IND0	GEN99_IND8	GEN99_IND16
1	0.4799	0.5265	0.5136	0.5456
2	0.4929	0.5498	0.5528	0.5624
3	0.5024	0.5687	0.5326	0.5323
4	0.5332	0.5387	0.5627	0.5325
5	0.5072	0.5365	0.5456	0.5510
6	0.5050	0.5265	0.5127	0.5325
7	0.5005	0.5515	0.5527	0.5312
8	0.5392	0.5502	0.5454	0.5688
9	0.5315	0.5463	0.5546	0.5368
10	0.5196	0.5451	0.5514	0.5329
11	0.5360	0.5514	0.5456	0.5412
12	0.5389	0.5564	0.5345	0.5445
13	0.5224	0.5798	0.5845	0.5312
Average	0.5161	0.5483	0.5453	0.5418

35.3.4 Excellent Genes Extraction

Each generation of individuals consists of a data column of five genomes to jointly determine the phenotypic characteristics. After fitting all the genomes of the 50 individuals of each generation to obtain the arithmetic mean, the representative values of the five genomes representing each generation are collected for statistical calculation and then compared with the genes of the six excellent individuals selected (Fig. 35.11), to find out the high score significant value relationship.

For the indicator of x division, the interquartile range is [2.06, 3.56] with a median of 3.13 and a mean of 3.08. The selected range of excellent genes is [2.92, 3.32], and the suitable division score is 3.0–3.3 after rounding upwards according to the division score characteristics. As the length range in the long side direction is [114, 120] for the study plot, the suitable building group length range in the long side direction for this study area is [34.54, 40.00].

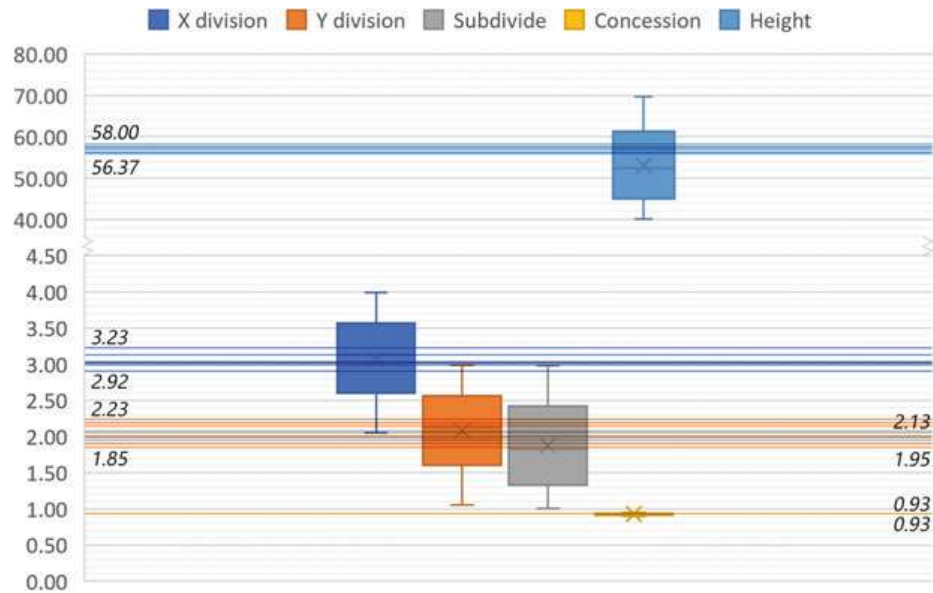
For the indicator of y division, the interquartile range is [1.60, 2.56] with a median of 2.13 and a mean of 2.08. The selected range of excellent genes is [1.85, 2.23], and the suitable division score is 1.9–2.2 after rounding upwards

according to the division score characteristics, which is basically equal to the average gene level. The length range in the short side direction to the study plot is [48, 65], and the suitable building group length range in the short side direction for this study area is [21.82, 34.21].

For the indicator of subdivide, the interquartile range is [1.33, 2.42] with a median of 1.82 and a mean of 1.87. The selected range of excellent genes is [1.95, 2.13], and the suitable value for the internal subdivision is 2 after rounding upwards according to the division score characteristics, which is above the average gene level. The suitable lengths in the long/short side directions for the study area are rounded, and the suitable length ranges in the two directions for the single building in this area are [17.27, 20.00] and [15.61, 17.10], respectively.

For the indicator of concession, the interquartile range is [0.91, 0.94] with a median of 0.92 and a mean of 0.93. The values of selected excellent genes are all 0.93, indicating that 93% is the global optimal solution for the indicator of building concession, which remains largely consistent with the mean and median gene levels. After fitting the better solution range of the long/short side division, the appropriate setback distances for this area are [4.84, 5.60] for

Fig. 35.11 Statistics of five types of input gene data and six excellent individual gene ranges



the length range in the long side direction and [3.05, 4.79] for the length range in the short side direction.

For the indicator of height, the interquartile range is [44.97, 61.31] with a median of 52.36 and a mean of 53.10. The selected range of excellent genes is [56.37, 58.00], which is significantly higher than the global gene level, and when combined with the floor heights, the suitable number of floors is approximately 17–20.

As a result, in Sham Shui Po and its surrounding areas, with the road network and block scale remaining unchanged, the following indicators for the renewal of the relevant buildings, based on the current situation of high-density development in Hong Kong and the AIP assessment context, are: in the direction of the long side of the site, the appropriate length of the building is 17.27–20.00 (m) and the appropriate concession distance is 4.84–5.60 (m); in the direction of the short side of the site, the appropriate length of the building is 15.61–17.10 (m) and the appropriate concession distance is 3.05–4.79 (m); the suitable number of floors of the building is 17–20. This data can provide a reference for future urban renewal or urban strategy implementation, and also can be used to re-extract excellent genes according to different optimization target orientations under renewal.

35.4 Conclusion and Future Works

This paper proposes a generic framework for the assessment and generation of urban building groups based on AIP. The assessment system is based on a literature review and provides a comprehensive quantification for urban exterior spaces, containing three levels of Safety, Accessibility & Mobility, and Comfort. The framework is able to avoid the acquisition of weights in subjective contexts through the CRITIC method in order to calculate comprehensive scores of AIP at different levels. At the same time, the combination of multi-objective optimization based on evolutionary algorithms can provide more permutation possibilities and obtain robustness after optimization by evolutionary algorithms at any time according to the goal orientation than the traditional top-down uniform planning. The proposed framework combines AIP evaluation, multi-source big data acquisition, spatial objective assignment and generation techniques under multi-objective optimization. It can be extended to other high-density urban areas in the field of age-appropriate urban space evaluation or urban renewal.

Meanwhile, the Pareto front solutions screened based on K-means in this paper demonstrate the advantages of unsupervised machine learning,

i.e., to quickly select clusters of different feature representations and to select central solutions. For the purpose of conducting future research on more iterations and more complex indicator systems, machine learning and reinforcement learning (RL) can be adopted to screen high-density solutions in evolutionary algorithms, where each individual can be considered as an agent with a reward function after objective selection, thus further accelerating optimization and achieving parallel optimal solutions.

Appendix

See Table 35.7.

Table 35.7 Glossary

Aging in Place (AIP)	The ability to live in one's own home and community safely, independently, and comfortably, regardless of age, income, or ability level
CRITIC method	One of the objective methods for determining the criteria weight
TPU planning range	The abbreviation of the third-level planning department of the Hong Kong Special Administrative Region
Jared Tarbell textures	Random subdivision texture
Multi-objective optimization	An area of multiple criteria decision making that is concerned with mathematical optimization problems involving more than one objective function to be optimized simultaneously
Evolutionary algorithm	An algorithm that uses mechanisms inspired by nature and solves problems through processes that emulate the behaviors of living organisms
Gene	Different input feature data for each individual in evolutionary algorithm
Population size	Iterative population size in evolutionary algorithm

(continued)

Table 35.7 (continued)

Aging in Place (AIP)	The ability to live in one's own home and community safely, independently, and comfortably, regardless of age, income, or ability level
Crossover probability	Gene (number) exchange probability in evolutionary algorithm
Mutation probability	Gene (number) mutation probability in evolutionary algorithm

References

- Buffel T, Handler S, Phillipson C (2018) Age-friendly cities and communities: A global perspective. Policy Press. <https://doi.org/10.2307/j.ctt1zrvhc4>
- Buffel T, Phillipson C, Rémillard-Boilard S (2019) Age-Friendly cities and communities: new directions for research and policy. In Gu D, Dupre M (Eds). Encycl Gerontol Popul AgingCham: Springer. https://doi.org/10.1007/978-3-319-69892-2_1094-1
- Dawidowicz A, Zysk E, Figurska M, Źróbek S, Kotnarowska M (2020) The methodology of identifying active aging places in the city—Practical application. Cities 98:102575. <https://doi.org/10.1016/j.cities.2019.102575>
- Deb K, Agrawal S, Pratap A, Meyarivan T (2000) A fast elitist non-dominated sorting genetic algorithm for multi-objective optimization: NSGA-II. In International Conference on Parallel Problem Solving from Nature (pp 849–858). Springer, Berlin, Heidelberg
- Gardner PJ (2011) Natural neighborhood networks—Important social networks in the public lives of older adults aging in place. J Aging Stud 25(3):236–271. <https://doi.org/10.1016/j.jaging.2011.03.007>
- Giridharan R, Lau SSY, Ganesan S, Givoni B (2007) Urban design factors influencing heat island intensity in high-rise high-density environments of Hong Kong. Build Environ 42(10):3669–3684. <https://doi.org/10.1016/j.buildenv.2006.09.011>
- Jayantha WM, Qian QK, Yi CO (2018) Applicability of ‘Aging in Place’ in redeveloped public rental housing estates in Hong Kong. Cities 83:140–151. <https://doi.org/10.1016/j.cities.2018.06.016>
- Jelokhani-Niaraki M, Hajiloo F, Samany NN (2019) A web-based public participation GIS for assessing the age-friendliness of cities: A case study in Tehran, Iran. Cities 95:102471. <https://doi.org/10.1016/j.cities.2019.102471>
- Kano M, Rosenberg PE, Dalton SD (2018) A global pilot study of age-friendly city indicators. Soc Indic Res 138(3):1205–1227. <https://doi.org/10.1007/s11205-017-1680-7>

- Lewis C, Buffel T (2020) Aging in place and the places of aging: A longitudinal study. *J Aging Stud* 54:100870. <https://doi.org/10.1016/j.jaging.2020.100870>
- Luciano A, Pascale F, Polverino F, Pooley A (2020) Measuring age-friendly housing: A framework. *Sustainability*, 12(3), 848. <https://doi.org/10.3390/su12030848>
- Makki M, Showkatbakhsh M, Song Y (2018) Wallacei: An evolutionary and Ana-lytic Engine for Grasshopper 3D. London, UK: Wallacei. <https://www.wallacei.com/>
- Mercader-Moyano P, Flores-García M, Serrano-Jiménez A (2020) Housing and neighbourhood diagnosis for ageing in place: Multidimensional Assessment System of the Built Environment (MASBE). *Sustain Cities Soc* 62:102422. <https://doi.org/10.1016/j.scs.2020.102422>
- Navarro-Mateu D, Makki M, Cocho-Bermejo A (2018) Urban-Tissue Optimization through Evolutionary Computation. *Math* 6(10):189. <https://doi.org/10.3390/math6100189>
- Peng S, Maing M (2021) Influential factors of age-friendly neighborhood open space under high-density high-rise housing context in hot weather: a case study of public housing in Hong Kong. *Cities* 115:103231. <https://doi.org/10.1016/j.cities.2021.103231>
- Planning Department. (2021) Projections of population distribution 2021–2029. <https://www.pland.gov.hk/index.html>
- Scharlach AE, Lehning AJ (2013) Ageing-friendly communities and social inclusion in the United States of America. *Ageing Soc* 33(1):110–136. <https://doi.org/10.1017/S0144686X12000578>
- World Health Organization (2022) Ageing and health. <https://www.who.int/news-room/fact-sheets/detail/ageing-and-health>
- Zhang F, Li D, Ahrentzen S, Zhang J (2019) Assessing spatial disparities of accessibility to community-based service resources for Chinese older adults based on travel behavior: A city-wide study of Nanjing, China. *Habitat International* 88:101984. <https://doi.org/10.1016/j.habitatint.2019.05.003>
- Zhang F, Chan APC, Darko A, Li D (2021) BIM-enabled multi-level assessment of age-friendliness of urban housing based on multiscale spatial framework: enlightenments of housing support for “aging-in-place.” *Sustain Cities Soc* 72:103039. <https://doi.org/10.1016/j.scs.2021.103039>